

Reducing the graphene grain density in three steps

This content has been downloaded from IOPscience. Please scroll down to see the full text.

2016 Nanotechnology 27 105602

(<http://iopscience.iop.org/0957-4484/27/10/105602>)

View [the table of contents for this issue](#), or go to the [journal homepage](#) for more

Download details:

IP Address: 140.116.20.22

This content was downloaded on 09/03/2017 at 13:19

Please note that [terms and conditions apply](#).

You may also be interested in:

[Effect of pressure and hydrogen flow in nucleation density and morphology of graphene bidimensional crystals](#)

S Chaitoglou and E Bertran

[Role of limited hydrogen and flow interval on the growth of single crystal to continuous graphene by low-pressure chemical vapor deposition](#)

Munu Borah, Abhishek K Pathak, Dilip K Singh et al.

[The role of hydrogen partial pressure on the annealing of copper substrates for graphene CVD synthesis](#)

Welyson T S Ramos, Thiago H R Cunha, Ingrid D Barcelos et al.

[Influence of the copper substrate roughness on the electrical quality of graphene](#)

Gi Duk Kwon, Eric Moyen, Yeo Jin Lee et al.

[Ultrasmooth metallic foils for growth of high quality graphene by chemical vapor deposition](#)

Pavel Procházka, Jindich Mach, Dominik Bischoff et al.

[Control of thickness uniformity and grain size in graphene films for transparent conductive electrodes](#)

Wei Wu, Qingkai Yu, Peng Peng et al.

[Rapid CVD growth of millimetre-sized single crystal graphene using a cold-wall reactor](#)

V Miseikis, D Convertino, N Mishra et al.

[Low temperature metal free growth of graphene on insulating substrates by plasma assisted chemical vapor deposition](#)

R Muñoz, C Munuera, J I Martínez et al.

Reducing the graphene grain density in three steps

Ya-Ping Hsieh¹, Yi-Hung Chu¹, He-Guang Tsai¹ and Mario Hofmann²

¹Graduate Institute of Opto-Mechatronics, National Chung Cheng University, 168 University Road, Min-Hsiung Township, Chiayi County 62102, Taiwan

²Department of Material Science and Engineering, National Cheng Kung University, Tainan 70101, Taiwan

E-mail: yphsieh@ccu.edu.tw and mario@mail.ncku.edu.tw

Received 19 November 2015, revised 25 December 2015

Accepted for publication 14 January 2016

Published 10 February 2016



CrossMark

Abstract

The production of large-scale, single crystalline graphene is a requirement for enhancing its electronic, mechanical, and chemical properties. Chemical vapor deposition (CVD) has shown the potential to grow high quality graphene but the simultaneous nucleation of many grains limits their achievable domain size. We report here that ultralow nucleation densities can be achieved through multi-step optimization of the catalyst morphology. First, annealing in a hydrogen-free environment is required to retain a surface copper oxide which decreases the nucleation density. Second, CuO was found to be the relevant copper species for this process and air oxidation of the copper foil at 200 °C maximizes its concentration. Both pre-treatment steps were found to affect the morphology of the catalyst and a direct correlation between nucleation density and surface roughness was found which indicates that the primary role of the oxidation step is the decrease in catalyst roughness. To further enhance this determining parameter, confined CVD was carried out after sample oxidation and hydrogen-free annealing. Each of these three steps reduces the grain density by approximately one order of magnitude resulting in ultralow nucleation densities of 1.23 grains/mm² and high quality, single-crystalline graphene grains of several millimeter sizes were grown using this method.

 Online supplementary data available from stacks.iop.org/NANO/27/105602/mmedia

Keywords: graphene, grain density, single crystalline, CVD

(Some figures may appear in colour only in the online journal)

1. Introduction

Graphene, a two-dimensional carbon allotrope [1, 2], has demonstrated significant potential in a multitude of research areas [3–5]. Many of these applications require the production of graphene at large scale and high quality. Chemical vapor deposition (CVD) is a promising approach to prepare high quality graphene on catalytic substrates [6–9]. One drawback of CVD growth is the poly-crystallinity of the graphene film with domain sizes ranging from nanometers to micrometers [10, 11]. The boundaries between grains will deteriorate its carrier transport [12], mechanical strength [10], thermal properties [13], and chemical inertness [14].

Consequently, the increase of graphene's domain size is a focus of significant attention [15–22]. Many promising approaches aim at decreasing the density of simultaneously growing graphene grains through minimization of the nucleation density. Reported approaches include thermal annealing [23, 24], electropolishing [25], and oxidation of copper foil prior to [19, 23] or during the CVD process [17]. The diversity of pretreatment methods indicates the lacking consensus on the mechanism responsible for decreasing the nucleation density. Eras *et al* suggested that the oxidation process removes organic impurities and surface contaminations thus affecting the growth kinetics [23]. Gan *et al* reported that the main effect of the oxidation is a change of

the catalyst morphology [16]. Finally, Hao *et al* proposed that the oxide layer changes the nucleation kinetics of the growth process [17].

We demonstrate that ultralow graphene nucleation densities can be achieved through a rational arrangement of several pretreatment steps that aim at controlling the catalyst morphology. First, the presence of copper oxide was found to result in a tenfold lowered nucleation density and hydrogen-free annealing conditions are required to retain it. Temperature-dependent air oxidation experiments furthermore reveal that CuO is the relevant copper oxide species for this nucleation control and optimization of its concentration yields an additional tenfold decrease in nucleation density. We identify the decrease in roughness upon oxidation as the underlying mechanism of this decrease. A direct proportionality between catalyst roughness and nucleation density was found irrespective of the details of the treatment processes. The catalyst roughness could be furthermore decreased by confined CVD which reduced the grain density by another order of magnitude. The demonstrated series of optimization steps helps to achieve a nucleation density of 1.23 grains/mm² which enables growth of millimeter-sized graphene domains. The domains exhibit single-crystallinity and high quality and demonstrate the potential of our method for the synthesis of graphene for future applications.

2. Experiment

Graphene was grown on copper foil (99.8%, Alfa-Aesar, no. 13382) following previous reports [26, 27]. Briefly, copper foil was first cleaned by electropolishing in a H₃PO₄ (85%) electrolyte at a potential of 2 V for 30 min. Oxidation of the copper foil on a hot plate was carried out for 30 min prior to CVD growth. CVD growth consisted of three process steps, heating, annealing, and growth. During the heating step, the reactor temperature was slowly raised to 1040 °C within 50 min under a flow of 320 sccm argon and a pressure of 1 Torr. Annealing was carried out at 1040 °C for 40 min under a flow of 320 sccm argon and 20 (or 0) sccm H₂ under a pressure of 1 Torr. The growth was conducted under a flow of 0.8 sccm CH₄ and 500 sccm H₂ for 80 min and at a pressure of 1 Torr. To visualize graphene on copper after synthesis samples were oxidized in air on a hot plate at 230 °C [25].

Image processing was used to analyze the grain density and grain size at 5 different positions within each sample and error bars represent the sample-to-sample variation. Atomic force microscopy was carried out on an AFM (E-7, Force Precision Instrument Co.) and roughness values represent the average of two 10 × 10 μm images. To quantify differences in morphology within each image, their line-to-line variations are represented as error bars.

For TEM measurements, graphene was transferred to TEM grids (TED PELLA 01881-F graphite lacey carbon) using PMMA as a mechanical support following established process parameters [28]. Raman spectroscopy was performed on a home-made micro-Raman system using 532 nm excitation wavelengths. Seven data points were taken for each

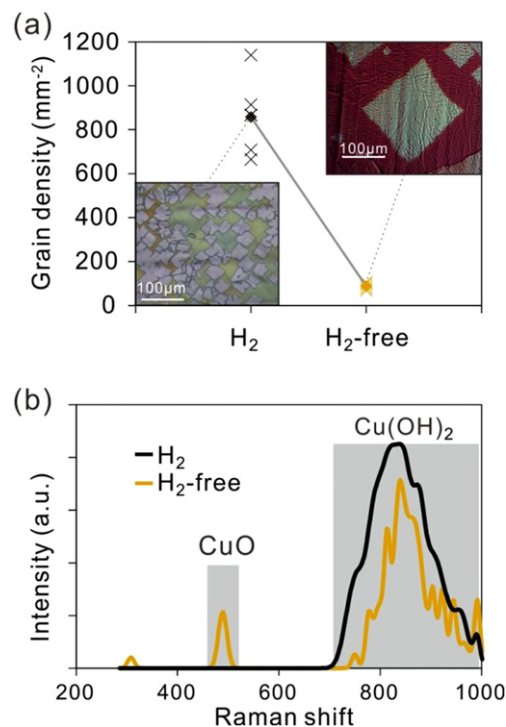


Figure 1. (a) Nucleation density of graphene grown after annealing under hydrogen-containing and hydrogen-free conditions, (b) Raman spectra of copper substrates after both annealing steps.

sample and each spectrum was fitted with Lorentzian peaks to obtain peak position and intensity information.

3. Results and discussion

A first step to identify the mechanism of oxidative copper pretreatment for graphene nucleation control is to establish at what growth stage the copper oxide has to be present. Previous explanations that cleaning of impurities is the main role of the oxidation step [23], for example, would only require the oxide to be present initially and then be consumed during the annealing stage. We therefore introduce two different annealing methods that differ by the process stage during which hydrogen is introduced. Common graphene growth procedures inject hydrogen during the annealing step [22]. We also carried out annealing without hydrogen to preserve the produced oxide layer. Figure 1(a) compares the average grain density of graphene grown under both annealing conditions. We observe that hydrogen-free annealing can decrease the nucleation density by more than one order of magnitude. This decrease in nucleation density results in larger achievable graphene domain sizes (insets of figure 1(a)) by limiting the interaction between neighboring graphene grains.

Raman characterization of the copper substrate after the different annealing procedures was carried out to investigate the origin of the decreased nucleation density (figure 1(b)). Two different Raman bands can be distinguished at 500 cm⁻¹, and 800 cm⁻¹. These features had previously been

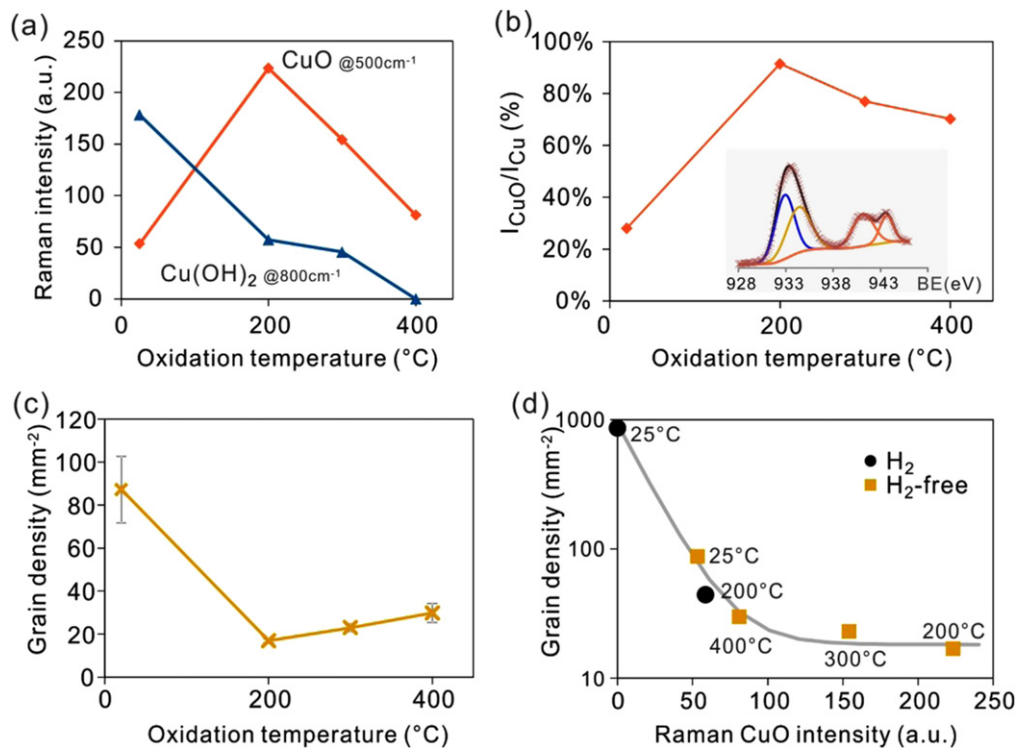


Figure 2. (a) Intensity of copper oxide Raman peaks after oxidation at different temperatures, (b) relative XPS peak intensity of CuO after oxidation at different temperatures, (inset) representative XPS spectrum of Cu 2p_{3/2} peak, (c) graphene grain density versus oxidation temperature, (d) grain density versus CuO peak intensity for different oxidation temperatures and annealing conditions (the gray line represents a least square fit as described in the main text).

assigned to CuO and Cu(OH)₂, respectively [29]. Comparison of the spectra for both annealing conditions confirms that the hydrogen atmosphere reduces the CuO but does not seem to affect the Cu(OH)₂, suggesting that the hydroxide is formed upon exposure to air. Hydrogen-free annealing, on the other hand, was found to retain CuO. We therefore conclude that the copper oxide has to be present after the annealing stage to reduce the grain density and hydrogen-free annealing conditions are required to retain it. To identify the role of copper oxides on the graphene nucleation, the concentration of copper oxides was varied by changing the oxidation temperature between 25 °C and 400 °C. Raman characterization shows that after annealing at 1000 °C the CuO concentration exhibits a maximum for samples that had been oxidized at 200 °C while the concentration of copper hydroxide decreases continuously with oxidation temperature (figure 2(a)). X-ray photoelectron spectroscopy was carried out to confirm this result. The Cu 2p_{3/2} peak and its shakeup were deconvoluted into contributions from pristine copper and CuO [30] (inset of figure 2(b)). The relative intensity of the CuO peak shows a similar trend to the results obtained by Raman spectroscopy which corroborates our finding.

The observed difference in the concentration and character of copper oxides can be used to identify correlations between pretreatment and nucleation. Figure 2(c) compares the nucleation density of graphene grown on copper foil that was air oxidized at different temperatures and subjected to hydrogen-free annealing. We observe that copper oxides grown at 200 °C show a lower nucleation density than Cu

oxides grown at higher temperatures. The strong correlation of the nucleation density with the concentration of the CuO phase indicates that this oxide phase affects graphene nucleation. A clear trend between the concentration of CuO after annealing and grain density is demonstrated in figure 2(d) and the grain density n can be completely predicted by the concentration of CuO through a simple exponential relation

$$n(c_{\text{CuO}}) = n_0 \exp(-\gamma c_{\text{CuO}}) + \eta,$$

where n_0 is the grain density at vanishing CuO concentrations ($n_0 \sim 850 \text{ mm}^{-2}$), γ is a proportionality constant ($\gamma \sim 0.05$), and η is the lowest achievable graphene grain density at full CuO coverage ($\eta \sim 17 \text{ mm}^{-2}$). The good fit of this model to the experimental data suggests that other details of the annealing process, such as oxidation temperature and hydrogen pressure only affect the nucleation density indirectly by modifying the CuO concentration.

To understand the reason for this correlation between CuO concentration and nucleation density, we carried out AFM characterization of the substrates after pre-treatment (figure 3(a)). We find that the oxidation of copper reduces the substrate roughness (figure 3(b)). This may be due to an enhanced evaporation of CuO compared to Cu [31] that leads to an improved surface recrystallization. Alternatively, the oxide might provide a protection against hydrogen-induced etching of the Copper surface which increases its roughness [16, 31]. The observed lower graphene nucleation density on those flatter substrates indicates that defects and protrusions

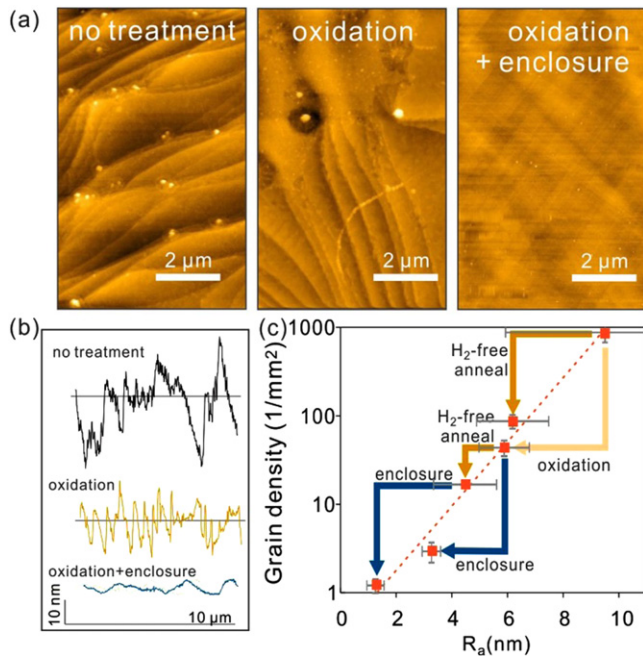


Figure 3. (a) AFM after different treatment steps, (b) representative cross-sections of the AFM images, (c) AFM-derived roughness R_a versus grain density for different combinations of treatments.

will act as nucleation centers and their reduction can control the graphene nucleation, in agreement with previous reports [32–34]. Consequently, the main effect of pre-treatment steps aiming at reducing the nucleation density is to decrease the substrate roughness.

Based on this theory, we expect that other approaches to reduce the copper roughness would also decrease the nucleation density. To test our hypothesis, we carry out confined CVD which has been reported to affect the copper evaporation process and result in a smoother copper surface [35]. A confinement effect was achieved by sandwiching a 2×7 cm piece of copper foil between two fused silica slides ($23 \times 75 \times 2$ mm, Xide Technology Ltd) and we indeed observe a decrease in the roughness after annealing (figure 3(b)). As predicted, the lowered roughness decreases the graphene nucleation density and a tenfold reduction between unconfined and confined CVD on oxidized Cu foil was found.

We quantified the roughness of the substrates by the arithmetic average of their absolute values R_a and demonstrate a direct proportionality between this roughness parameter and the nucleation density (figure 3(c)). The effectiveness of each pretreatment step in reducing the graphene grain density (supplementary figure S1, available at stacks.iop.org/NANO/27/105602/mmedia) was found to be primarily determined by its ability to reduce the substrate roughness. This observation is in contrast to previous reports that suggested the impact of CuO sites on the growth kinetics [17]. Instead, we find no correlation between the graphene growth rate and the grain density (supplementary figure S2). This observation is

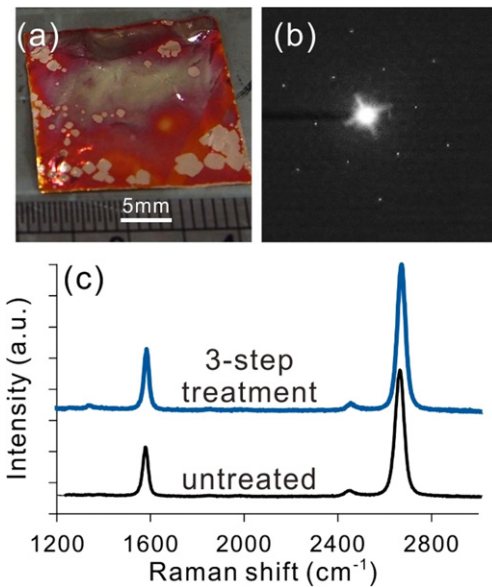


Figure 4. (a) Photograph of 1.5×1.5 cm copper sample after air oxidation exhibiting ultralow graphene grain density, (b) selected area electron diffraction (SAED) image of transferred single grain, (c) Raman I_D/I_G ratio for graphene grown on untreated and treated copper.

in agreement with recent reports about the similarity in the graphene growth kinetics on Cu and CuO [36].

The observed exponential dependence of grain density on substrate roughness furthermore suggests the sensitivity of graphene growth on the substrate morphology. The grain density was minimized by combining all three treatment steps—oxidation, hydrogen free annealing, and confined CVD growth. The resulting grain density of 1.23 mm^{-2} is an average over many centimeter-sized samples and is repeatable and stable. Further reduction in grain density could be achieved in the future by optimizing the growth process [23].

Using this method, we produced millimeter-scale graphene grains (figure 4(a)). The difference in grain size was found to be caused by a transport-limited growth process which is not affecting the grain density [37]. Selected area electron diffraction (SAED) shows that each of the millimeter-sized graphene grains is single crystalline (figure 4(b)). Furthermore, Raman characterization suggests that the produced graphene is of a quality that is comparable to unenclosed and non-oxidized growth as indicated by the absence of the defect-related D-band (figure 4(c)).

4. Conclusion

In conclusion, we provide a route to achieve ultralow graphene nucleation densities by combining three steps that aim at controlling the catalyst morphology. First, the formation of copper oxide is a requirement for low nucleation density and hydrogen-free annealing conditions are needed. The oxidation at 200°C results in the highest concentration of CuO phase and the lowest achievable grain density indicating that the

selectivity of the nucleation process to a certain copper oxide species. A direct proportionality between substrate roughness and nucleation density was found which implies that the main role of the oxidation step is the reduction of substrate roughness. Based on this finding confined CVD growth was used to further reduce the substrate roughness and an additional tenfold decrease in the nucleation density was observed.

The graphene nucleation density after combining all three treatment steps is three orders of magnitude lower than for traditional graphene growth and reaches 1.23 grains/mm². This method can be applied to produce high quality macroscopic single crystals of graphene at large scale to facilitate the use of CVD graphene in high performance applications.

Acknowledgments

YP Hsieh and M Hofmann acknowledges financial support from Applied Materials, Inc., the Ministry of Science and Technology (102-2112-M-194-003-MY3, and 104-2112-M-006-013-MY3), and the Industrial Technology Research Institute of Taiwan.

References

- [1] Novoselov K S, Geim A K, Morozov S V, Jiang D, Katsnelson M I, Grigorieva I V, Dubonos S V and Firsov A A 2005 Two-dimensional gas of massless dirac fermions in graphene *Nature* **438** 197–200
- [2] Novoselov K S, Geim A K, Morozov S V, Jiang D, Zhang Y, Dubonos S V, Grigorieva I V and Firsov A A 2004 Electric field effect in atomically thin carbon films *Science* **306** 666–9
- [3] Ferrari A C *et al* 2015 Science and technology roadmap for graphene, related two-dimensional crystals, and hybrid systems *Nanoscale* **7** 4598–810
- [4] Geim A K and Novoselov K S 2007 The rise of graphene *Nat. Mater.* **6** 183–91
- [5] Zhang Y, Tan Y-W, Stormer H L and Kim P 2005 Experimental observation of the quantum hall effect and berry's phase in graphene *Nature* **438** 201–4
- [6] Bae S *et al* 2010 Roll-to-roll production of 30-inch graphene films for transparent electrodes *Nat. Nanotechnol.* **5** 574–8
- [7] Kim K S *et al* 2009 Large-scale pattern growth of graphene films for stretchable transparent electrodes *Nature* **457** 706–10
- [8] Li X S *et al* 2009 Large-area synthesis of high-quality and uniform graphene films on copper foils *Science* **324** 1312–4
- [9] Reina A, Jia X T, Ho J, Nezich D, Son H B, Bulovic V, Dresselhaus M S and Kong J 2009 Large area, few-layer graphene films on arbitrary substrates by chemical vapor deposition *Nano Lett.* **9** 30–5
- [10] Huang P Y *et al* 2011 Grains and grain boundaries in single-layer graphene atomic patchwork quilts *Nature* **469** 389–92
- [11] Tsen A W *et al* 2012 Tailoring electrical transport across grain boundaries in polycrystalline graphene *Science* **336** 1143–6
- [12] Cummings A W, Duong D L, Nguyen V L, Tuan D V, Kotakoski J, Vargas J E B, Lee Y H and Roche S 2014 Charge transport in polycrystalline graphene: challenges and opportunities *Adv. Mater.* **26** 5079–94
- [13] Yu Q K *et al* 2011 Control and characterization of individual grains and grain boundaries in graphene grown by chemical vapour deposition *Nat. Mater.* **10** 443–9
- [14] Hsieh Y-P, Hofmann M, Chang K-W, Jhu J G, Li Y-Y, Chen K Y, Yang C C, Chang W-S and Chen L-C 2014 Complete corrosion inhibition through graphene defect passivation *ACS Nano* **8** 443–8
- [15] Zhou H L *et al* 2013 Chemical vapour deposition growth of large single crystals of monolayer and bilayer graphene *Nat. Commun.* **4** 8
- [16] Gan L and Luo Z T 2013 Turning off hydrogen to realize seeded growth of subcentimeter single-crystal graphene grains on copper *ACS Nano* **7** 9480–8
- [17] Hao Y F *et al* 2013 The role of surface oxygen in the growth of large single-crystal graphene on copper *Science* **342** 720–3
- [18] Li J, Wang X-Y, Liu X-R, Jin Z, Wang D and Wan L-J 2015 Facile growth of centimeter-sized single-crystal graphene on copper foil at atmospheric pressure *J. Mater. Chem. C* **3** 3530–5
- [19] Li X S, Magnuson C W, Venugopal A, Tromp R M, Hannon J B, Vogel E M, Colombo L and Ruoff R S 2011 Large-area graphene single crystals grown by low-pressure chemical vapor deposition of methane on copper *J. Am. Chem. Soc.* **133** 2816–9
- [20] Wang C C *et al* 2014 Growth of millimeter-size single crystal graphene on cu foils by circumfluence chemical vapor deposition *Sci. Rep.* **4** 5
- [21] Wang H, Wang G Z, Bao P F, Yang S L, Zhu W, Xie X and Zhang W J 2012 Controllable synthesis of submillimeter single-crystal monolayer graphene domains on copper foils by suppressing nucleation *J. Am. Chem. Soc.* **134** 3627–30
- [22] Yan Z *et al* 2012 Toward the synthesis of wafer-scale single-crystal graphene on copper foils *ACS Nano* **6** 9110–7
- [23] Eres G, Regmi M, Rouleau C M, Chen J, Ivanov I N, Puzos A A and Geoghegan D B 2014 Cooperative Island growth of large-area single-crystal graphene on copper using chemical vapor deposition *ACS Nano* **8** 5657–69
- [24] Gan L and Luo Z 2013 Turning off hydrogen to realize seeded growth of subcentimeter single-crystal graphene grains on copper *ACS Nano* **7** 9480–8
- [25] Luo Z T, Lu Y, Singer D W, Berck M E, Somers L A, Goldsmith B R and Johnson A T C 2011 Effect of substrate roughness and feedstock concentration on growth of wafer-scale graphene at atmospheric pressure *Chem. Mater.* **23** 1441–7
- [26] Hsieh Y P, Hofmann M and Kong J 2014 Promoter-assisted chemical vapor deposition of graphene *Carbon* **67** 417–23
- [27] Li X *et al* 2009 Large-area synthesis of high-quality and uniform graphene films on copper foils *Science* **324** 1312–4
- [28] Li X, Zhu Y, Cai W, Borysiak M, Han B, Chen D, Piner R D, Colombo L and Ruoff R S 2009 Transfer of large-area graphene films for high-performance transparent conductive electrodes *Nano Lett.* **9** 4359–63
- [29] Roy S S and Arnold M S 2013 Improving graphene diffusion barriers via stacking multiple layers and grain size engineering *Adv. Funct. Mater.* **23** 3638–44
- [30] Wu C-K, Yin M, O'Brien S and Koberstein J T 2006 Quantitative analysis of copper oxide nanoparticle composition and structure by x-ray photoelectron spectroscopy *Chem. Mater.* **18** 6054–8
- [31] Mack E, Osterhof G G and Kraner H M 1923 Vapor pressure of copper oxide and of copper *J. Am. Chem. Soc.* **45** 617–23
- [32] Han G H, Güneş F, Bae J J, Kim E S, Chae S J, Shin H-J, Choi J-Y, Pribat D and Lee Y H 2011 Influence of copper morphology in forming nucleation seeds for graphene growth *Nano Lett.* **11** 4144–8

- [33] Magnuson C W, Kong X, Ji H, Tan C, Li H, Piner R, Ventrice C A and Ruoff R S 2014 Copper oxide as a 'self-cleaning' substrate for graphene growth *J. Mater. Res.* **29** 403–9
- [34] Strudwick A J, Weber N E, Schwab M G, Kettner M, Weitz R T, Wunsch J R, Müllen K and Sachdev H 2015 Chemical vapor deposition of high quality graphene films from carbon dioxide atmospheres *ACS Nano* **9** 31–42
- [35] Chen S S *et al* 2013 Millimeter-size single-crystal graphene by suppressing evaporative loss of Cu during low pressure chemical vapor deposition *Adv. Mater.* **25** 2062–5
- [36] Gottardi S *et al* 2015 Comparing graphene growth on Cu(111) versus oxidized Cu(111) *Nano Lett.* **15** 917–22
- [37] Hsieh Y-P, Shih C-H, Chiu Y-J and Hofmann M 2016 High-throughput graphene synthesis in gapless stacks *Chem. Mater.* **28** 40–43